

https://dspace.org/

A polarographic and potentiometric study of metal-ligand equilibria: Instrumentation and investigations of systems with non-reversible electrode reactions

Mkwizu, Tumaini Samuel Peter

2006-11-13T13:05:09Z
http://hdl.handle.net/10539/1647

Downloaded from a DSpace repository. https://dspace.org/

CHAPTER 3

THEORY AND TREATMENT OF DATA

3.1 INTRODUCTION

This chapter describes the various methodologies adopted for analysis of experimental data collected in this project. Relevant theoretical background on the methodologies used is also highlighted. Firstly, methodologies for treatment and analysis of glass electrode potentiometric data, used in determination of protonation and stability constants for the ligands and metal–ligand systems studied are discussed. Secondly, treatment of polarographic data in modelling and refinement of stability constants is presented. Finally, models adopted from literature, and tested in this project, for use in analysis of DC polarographic curves, from studies of metal–ligand systems with varying electrochemical reversibility, are discussed.

3.2 GLASS ELECTRODE POTENTIOMETRIC STUDIES: THEORY, MODELLING AND REFINEMENT OF PROTONATION AND STABILITY CONSTANTS

In elucidation of the equilibrium model for a given system, one is confronted with three major aspects: (a) the selection of the best of several plausible equilibrium models; (b) the estimation of stability constants and other parameters related to the particular equilibrium model; and (c) the calculation of distribution diagrams for all species over the range of experimental conditions [1].

Potentiometry is often used as a technique to calculate stability constants and determine protonation constants. In these regards, potentiometric studies are based primarily on measurements of at least one of the species involved in protonation or metal–ligand equilibria. The essence of the potentiometric experiment involving a glass electrode is the monitoring of the change in the hydrogen ion concentration, $[H^+]$, throughout the experiment. The experimentally known

quantities in a potentiometric titration are: (a) the initial analytical concentrations (commonly referred to as total concentrations) of the reactants in the solution; (b) the added volumes of the titrant solution of known concentration; and (c) the free concentration of one (or more) reactants in the solution, *e.*g., $[H^+]$ in the case of Glass Electrode Potentiometry (GEP), which implies previous calibration of the potentiometric cell [2–3].

For a protic ligand *L* with a maximum of *m* protons that can participate in protonation equilibria, the overall protonation constant (β_m^H) can be written as:

$$mH + L \leftrightarrow H_mL \qquad \beta_m^H = \frac{[H_mL]}{[L][H]^m} \qquad \textbf{(3.1)}$$

When a metal ion *M* is involved in complexation reactions with the ligand *L*, the overall concentration stability constant, $\beta_{M_pL_qH_r}$, of the complex $M_pL_qH_r$ is defined by:

$$pM + qL + rH \leftrightarrow M_pL_qH_r \qquad \beta_{M_pL_qH_r} = \frac{[M_pL_qH_r]}{[M]^p[L]^q[H]^r} \qquad \textbf{(3.2)}$$

In aqueous media, there is always equilibrium between H^+, OH^-, and H_2O, which is governed by the ionic product, K_w:

$$H^+ + OH^- \leftrightarrow H_2O \qquad K_w = [H^+][OH^-] \qquad \textbf{(3.3)}$$

In Equations 3.1 and 3.2, and the remainder of this chapter charges in the equilibrium reactions are omitted for clarity.

In order to calculate protonation or stability constants from potentiometric data, appropriate mass balance equations (MBEs) are needed. Three MBEs are usually considered: total ligand concentration, $[L_T]$, total hydrogen ion concentration, $[H_T]$, and total metal ion concentration, $[M_T]$. Equations 3.4 to 3.6 represent the

general form of MBEs. All three equations are considered in a study of a metal–ligand system by GEP. For determination of protonation constants for a ligand, only the mass balance equations for $[L_T]$ and $[H_T]$ are considered and $M_pL_qH_r$ species would simply be H_rL_q.

$$[L_T] = [L] + \sum_q q\beta_{M_pL_qH_r}[M_pL_qH_r] \quad \textbf{(3.4)}$$

$$[M_T] = [M] + \sum_p p\beta_{M_pL_qH_r}[M_pL_qH_r] \quad \textbf{(3.5)}$$

$$[H_T] = [H^+] - [OH^-] + \sum_r r\beta_{M_pL_qH_r}[M_pL_qH_r] \quad \textbf{(3.6)}$$

In order to estimate the unknown parameters (e.g., the stability constants) using potentiometric titration data and the relevant mass balance equations, the least–squares method is used. In this procedure, the simultaneous optimization of the unknown parameters is achieved through minimization of an objective function, *U*, defined in general as:

$$U = \sum_i w_i (y_i^{obs} - y_i^{calc})^2 \quad \textbf{(3.7)}$$

where y_i^{obs} are the experimentally observed quantities (could be either total concentration of H^+ at *i*th titration point or emf of electrode at *i*th point) and y_i^{calc} are the corresponding calculated values, by means of a functional relationship which is assumed to be known; w_i are the weights of each observation *i*.

The mathematical problem is that of finding the numerical values of the stability constants which will minimize *U* subject to the constraints imposed by Equations 3.3–3.6 for each titration point, starting with reasonable estimates of the unknown stability constants. The unknown stability constants are then adjusted and the

calculations are repeated until no further minimization of U is obtained, thus providing the final calculated β values for the assumed model. The computational method is necessarily tedious and digital computers, with appropriate programs, are employed to perform the optimization procedures [4–5].

Although the evaluation of the potentiometric data can be handled by different software packages, in this study the GEP data were analysed using the more robust ESTA (Equilibrium Simulation by Titration Analysis) suite of computer programs [6–8]. ESTA imposes the conditions of mass balance in the standard way by equating calculated total concentrations with real (analytical) concentrations. The Gauss–Newton and Levenberg–Marquardt algorithms are used in ESTA for minimization of the objective function U (Equation 3.7). ESTA accommodates chemical systems of up to 10 components forming up to 99 complexes. Titrations involving up to three electrodes and three burettes are permitted. The programs can take into account variations in ionic strength and the associated changes in activity coefficients. They also permit corrections of titration data affected by liquid–junction potentials and imperfect ion–selectivity of electrodes.

The ESTA library contains program modules, which perform one or more kinds of calculations (specified as different 'tasks'). ESTA1 and ESTA2 modules have been used extensively in this project. A brief discussion of these modules is given here.

ESTA1: The simulation module

By setting up and solving the mass balance equations, ESTA1 can determine, on a point–by–point basis, single values for almost any titration parameter. The calculations fall into two categories: (i) species–distribution calculations and (ii) potentiometric titration calculations. The latter includes emf values, stability constant estimates, total analytical concentrations, initial vessel concentrations and initial burette concentrations. This program is commonly used to generate

formation function values (task *ZBAR*), deprotonation function values (task *QBAR*) and protonation values (task *NBAR*).

The *ZBAR* task was used for modelling of GEP data in this study. In determination of protonation constants the protonation formation function *ZBAR(H)* is very useful in prediction of the number of protonation steps and the corresponding initial estimates directly from the experimental data. *ZBAR(H)* depends only on pH, hence, *ZBAR(H)* is plotted against pH and from such plots one can extract such information as the number of protonation equilibria predicted from the experimental data. *ZBAR(H)* can be interpreted as the average number of protons coordinated per ligand molecule at any titration point and is defined as:

$$ZBAR(H) = \frac{[H_T] - [H^+] + [OH^-]}{[L_T]} \qquad \textbf{(3.8)}$$

where $[H_T]$ and $[L_T]$ are total concentrations of protons and ligand, as defined in Equations 3.6 and 3.4, respectively.

Another useful formation function is *ZBAR(M)*, the metal complexes formation function. *ZBAR(M)* can be described as the number of ligands bound per metal ion at a certain titration point. The explicit definition of *ZBAR(M)* is:

$$ZBAR(M) = \frac{[L_T] - [L]}{[M_T]} \qquad \textbf{(3.9)}$$

where [L] is the concentration of free ligand at a specific titration point, $[L_T]$ and $[M_T]$ have their usual meanings as defined by Equations 3.4 and 3.5.

ZBAR(M) depends on [L] and is plotted against pL = –Log [L]. By using the ESTA1 module, graphs can be drawn of *ZBAR(H)* versus pH or *ZBAR(M)* versus pL, where the observed and calculated functions can be compared and electrode potentials (observed and calculated) evaluated respectively. If the calculated and

observed curves match each other closely in the pH (or pL) region of interest, the proposed model and formation constants can be regarded as plausible.

ESTA2: The optimization module

Within ESTA2, there are two optimisation programs; ESTA2A and ESTA2B, differing only in the way data are weighted. They are used when it is desired to determine, for one or more parameters, the 'best' values, based on a least–square procedure applied to a whole system of titrations. In this way the following parameters can be refined: stability constants, vessel and burette concentrations, electrode parameters (E^k and response slope s), and initial vessel volume. It is possible to group together, over any combinations of titrations, local parameters of the same type with the same value so that they are refined together as a single parameter. The approach is to refine the stability constants with ESTA2 until the best values for the statistical parameters (standard deviations and Hamilton factors) are reached. After this, the proposed model of stability constants is evaluated by *QBAR* or *ZBAR* comparisons of observed against the calculated data from final values obtained from refinement of a given model.

3.3 SAMPLED DIRECT CURRENT POLAROGRAPHIC STUDIES: THEORY, MODELLING AND REFINEMENT OF STABILITY CONSTANTS

3.3.1 Optimisation of a Metal–Ligand Model and Refinement of Stability Constants

The refinement operations and modelling of DC polarographic data were performed using the Cukrowski method of speciation [9–14]. This method uses mass balance equations written for fully–labile, inert or mixed metal–ligand systems with the requirement that the processes observed are electrochemically reversible on the polarographic timescale employed. The methodology was adopted in analysis of metal–ligand systems studied in this project by sampled

Direct Current Polarography (DCP) at a fixed total ligand to total metal ion concentration ratio and varied pH. The methodology is based on Equation 3.10.

$$\left(E_{1/2}(\mathrm{M}) - \left(E_{1/2}(\mathrm{comp})\right)_{pH(i)}\right) - \frac{RT}{nF}\ln\left(\frac{I(\mathrm{comp})}{I(\mathrm{M})}\right)_{pH(i)} = \frac{RT}{nF}\ln\left(\frac{[\mathrm{M_T}]}{[\mathrm{M}]}\right)_{pH(i)} \qquad \textbf{(3.10)}$$

In Equation 3.10, $E_{1/2}$(M) and I(M) stand for the half–wave potential ($E_{1/2}$) and limiting–diffusion current (I_d) recorded in a polarographic experiment in the absence of metal–ligand complexes; $E_{1/2}$(comp) and I(comp) stand for the half–wave potential and limiting–diffusion current obtained from the *i*th polarogram in the presence of metal–ligand complexes at *i*th pH. The left–hand side of Equation 3.10 is calculated directly from experimental data provided that $E_{1/2}$(M) is available from the experiment. The plot of the left–hand side of Equation 3.10 versus pH generates the Experimental Complex Formation Curve (ECFC). The ECFC is used as the experimental objective function that has to be reproduced by a theoretical function, the Calculated Complex Formation Curve (CCFC), *i.e.*, the right–hand side of Equation 3.10. The refinement of stability constants is achieved by the computation of the free–metal–ion concentration [M] from mass balance equations written for the assumed model. The computed [M] is used by the right–hand side of Equation 3.10. During the iterative operation, the values of refined stability constants are varied. The refinement operation is completed when the CCFC fits best the experimental objective function, *i.e.*, the ECFC.

The total metal ion and ligand concentrations, [M_T] and [L_T], are known at any stage of the experiment. Appropriate mass balance equations can be written for the total concentrations of metal ion and ligand as is the case in refinement of potentiometric data (see Equations 3.4–3.5). To illustrate the refinement procedure employed for metal–ligand systems studied, consider the following metal–ligand model: ML, ML_2, and ML_3. The metal ion is M^{2+} and the ligand is L^-, with two protonation constants. In development of relevant mass balance equations, in addition to the metal–ligand species being considered, all known metal complexes involving OH^- should be included in the model. For illustration

purposes the following species are assumed to be known: $M(OH)$, $M(OH)_2$, $M(OH)_3$, $M(OH)_4$, $M_2(OH)$, and $M_4(OH)_4$. The mass balance equations are given in Equations 3.11–3.12.

$$\begin{aligned}[M_T] = [M] &+ \beta_{ML}[M][L] + \beta_{ML_2}[M][L]^2 + \beta_{ML_3}[M][L]^3 + \beta_{M(OH)}[M][OH] \\ &+ \beta_{M(OH)_2}[M][OH]^2 + \beta_{M(OH)_3}[M][OH]^3 + \beta_{M(OH)_4}[M][OH]^4 \\ &+ 2\beta_{M_2(OH)}[M]^2[OH] + 4\beta_{M_4(OH)_4}[M]^4[OH]^4\end{aligned} \quad \textbf{(3.11)}$$

$$\begin{aligned}[L_T] = [L] &+ K_1^H[H][L] + K_1^H K_2^H[H]^2[L] + \beta_{ML}[M][L] + 2\beta_{ML_2}[M][L]^2 \\ &+ 3\beta_{ML_3}[M][L]^3\end{aligned} \quad \textbf{(3.12)}$$

where K_n^H stand for the stepwise protonation constants of the ligand, β_{ML_q} stand for the overall stability constants, [M], [L], [H], and [OH] stand for the free metal ion, free ligand, hydrogen, and hydroxide ion concentrations, respectively. During the refinement procedure, the stepwise protonation constants of the ligand and the hydrolysis constants of the metal ion are kept fixed, since they would typically be known from previous studies.

The refinement procedure employed in this work followed the following steps. One starts with initial guesses for the values of stability constants $\beta_{ML}, \beta_{ML_2}, \beta_{ML_3}$, etc. Equations 3.11 and 3.12 must hold at any stage of the experimental procedure (*e.g.*, after each addition of the standardized NaOH solution) and can be written in a simplified form as Equations 3.13 and 3.14, where *exp* and *calc* stand for experimental and calculated values.

$$\{[M_T]_{(exp)}\}_{pH(i)} = \{[M_T]_{(calc)}\}_{pH(i)} \quad \textbf{(3.13)}$$

$$\{[L_T]_{(exp)}\}_{pH(i)} = \{[L_T]_{(calc)}\}_{pH(i)} \quad \textbf{(3.14)}$$

Equations 3.13 and 3.14 are solved iteratively at each pH(*i*) value simultaneously (with particular values of refined stability constants) for the free–metal–ion and

free–ligand concentrations. The free–metal–ion concentration obtained at each iteration step is then used in the right–hand side of Equation 3.10. The computed [M] is used by the right–hand side of Equation 3.10. During the iterative operation, the values of refined stability constants are varied. The refinement operation is completed when the CCFC fits best the experimental objective function, *i.e.*, the ECFC. The goodness-of-fit is judged by the overall fit (OF) computed using Equation 3.15).

$$OF = \sqrt{\frac{\sum (\mathrm{ECFC} - \mathrm{CCFC})^2_{pH(i)}}{k-1}} \ [mV] \qquad \textbf{(3.15)}$$

where k stands for the total number of experimental points.

It is to be noted that the refinement operations employed in the evaluation of polarographic data do not include the mass balance equation for the total hydrogen ion concentration [H_T]. This is the fundamental difference between the polarographic and potentiometric theories and mathematical procedures employed. The free–hydrogen or hydroxide ion concentrations ([H^+] and [[OH^-]) are obtained directly from the pH measurements by the calibrated glass electrode and K_w for water. The optimization of a given model and refinement of stability constants were carried out with a dedicated computer software *3D Complex Formation Curves* (*3D–CFC*) [15].

3.3.2 General Concepts in Modelling of Polarographic Data

3.3.2.1 Variation in Half–Wave Potential as a function of pH

It has been demonstrated that a plot of the observed half–wave potential, $E_{1/2}$ of a labile DC wave (or peak potential in the case of Differential Pulse Polarography) versus pH, such as the one seen in Figure 3.1, can be used for prediction of major labile[1] metal complexes [11, 16–17]. A slope of about $r(RT/nF)/p$ (where r, n, and

[1] Labile species are those species that have fast exchange rate between the metal ion and its ligand relative to the timescale of the measuring technique, i.e., fast homogeneous kinetics [11]

p stand for the number of protons, electrons and metal ions involved in the overall electrochemical reaction, respectively; *R*, *T*, and *F* have their usual meanings) can be expected when labile metal complexes are formed in a specific pH range where there is a predominant ligand species. This means that when one metal complex is predominant in the pH range where one form of a ligand also dominates, then a slope of about 59.16/*n* mV per pH unit and per proton involved in the electrochemical reaction is observed at 25 °C, provided that polynuclear metal containing species are not formed ($p = 1$).

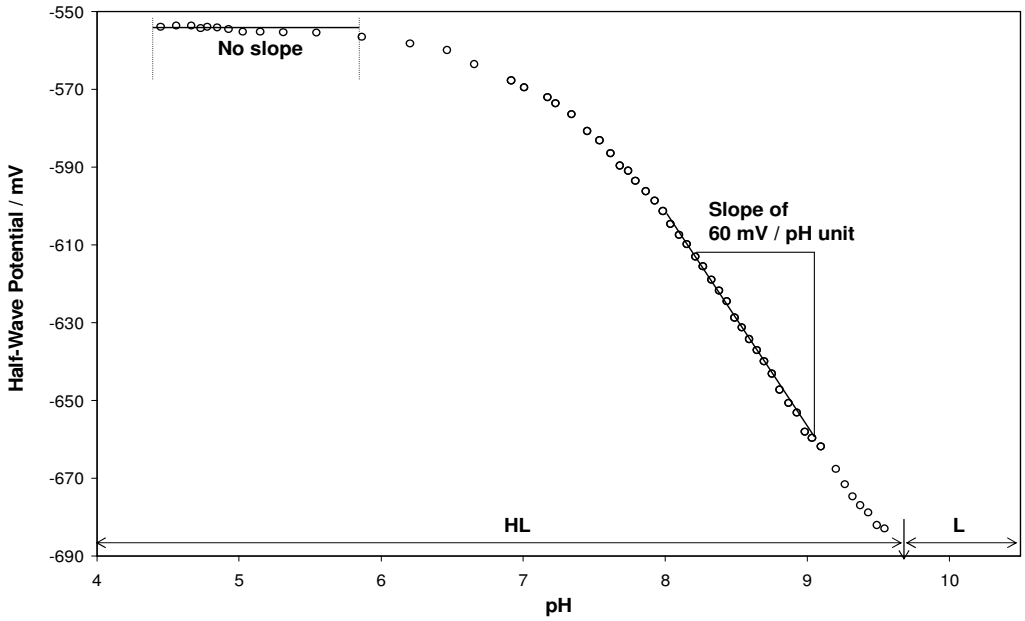


Figure 3.1: A typical relationship of variation in half–wave potential for Cd^{2+}, in the presence of the protic ligand glycine, as a function of pH.

The change in the slope is caused by: (i) the change in the predominant form of the ligand in the solution and (ii) change in the predominant form of the metal species as a result of different number of protons being involved in the overall electrochemical process occurring at the DME. To illustrate the use of such slopes, some examples of plausible electrochemical processes are given here.

In general, the major electrochemical process at the DME involving a ligand and a bivalent metal ion (such as cadmium or lead) could be (charges are omitted for simplicity):

$$M(HL) + H + 2e \leftrightarrow M(Hg) + H_2L \qquad \text{(1 proton)} \qquad \textbf{(3.16)}$$

or

$$ML + 2e + 2H \leftrightarrow M(Hg) + H_2L \qquad \text{(2 protons)} \qquad \textbf{(3.17)}$$

for the predominant ligand form H_2L, and

$$M(HL) + 2e \leftrightarrow M(Hg) + HL \qquad \text{(no proton)} \qquad \textbf{(3.18)}$$

or

$$ML + 2e + H \leftrightarrow M(Hg) + HL \qquad \text{(1 proton)} \qquad \textbf{(3.19)}$$

or in general,

$$ML_q + 2e + qH \leftrightarrow M(Hg) + qHL \qquad \text{(q protons)} \qquad \textbf{(3.20)}$$

for the predominant HL form of the ligand.

There are no protons involved in the electrochemical process depicted in Equation 3.18 (shift in $E_{1/2} \approx 0$). The plot given in Figure 3.1 provides a good example of such a situation in the pH range 4 to 6. This could be interpreted as formation of M(HL) species or no complexation takes place in the pH range considered.

Equations 3.16 and 3.19 require the involvement of one proton. From Equations 3.16 and 3.19 a slope of about 29 mV per pH unit should be observed on the plot of $E_{1/2}$ versus pH at the appropriate pH values. Similarly, for complexes in which two protons are involved in the electrochemical processes at the DME, a slope of about 59 mV per pH unit would be expected. In Figure 3.1, a slope of about 60 mV per pH unit is observed in the pH range 7.5 to 9. This might indicate existence of the ML_2 species (Equation 3.20). When no protons are involved in the electrochemical reaction, the slope approaches null. This could be observed at low pH, where a reaction such as that given in Equation 3.18 might occur or in the pH regions where the ligand exists as free (fully–deprotonated) ligand and the following reactions would be considered:

$$ML_q + 2e \leftrightarrow M(Hg) + qL \qquad \text{(no protons)} \qquad \textbf{(3.21)}$$

3.3.2.2 Variation in Half–Wave Potential versus free ligand concentration

The formation of the species ML_j can often be confirmed from the relationship of the observed shift in the half–wave potential against free ligand concentration [L] (expressed as Log [L]). If a Nernstian slope is observed in a specific free ligand concentration range, then it is possible to identify species such as ML, ML_2, ML_3, …, ML_q. For a bivalent metal ion such as cadmium, the following equilibrium relations should hold (charges omitted for clarity)

$$M + L \leftrightarrow ML \qquad \text{slope} \approx 30 \text{ mV per Log unit} \qquad \textbf{(3.22)}$$

$$M + 2L \leftrightarrow ML_2 \qquad \text{slope} \approx 60 \text{ mV per Log unit} \qquad \textbf{(3.23)}$$

or in general,

$$M + qL \leftrightarrow ML_q \qquad \text{slope} \approx q(59.16/2) \text{ per Log unit} \qquad \textbf{(3.24)}$$

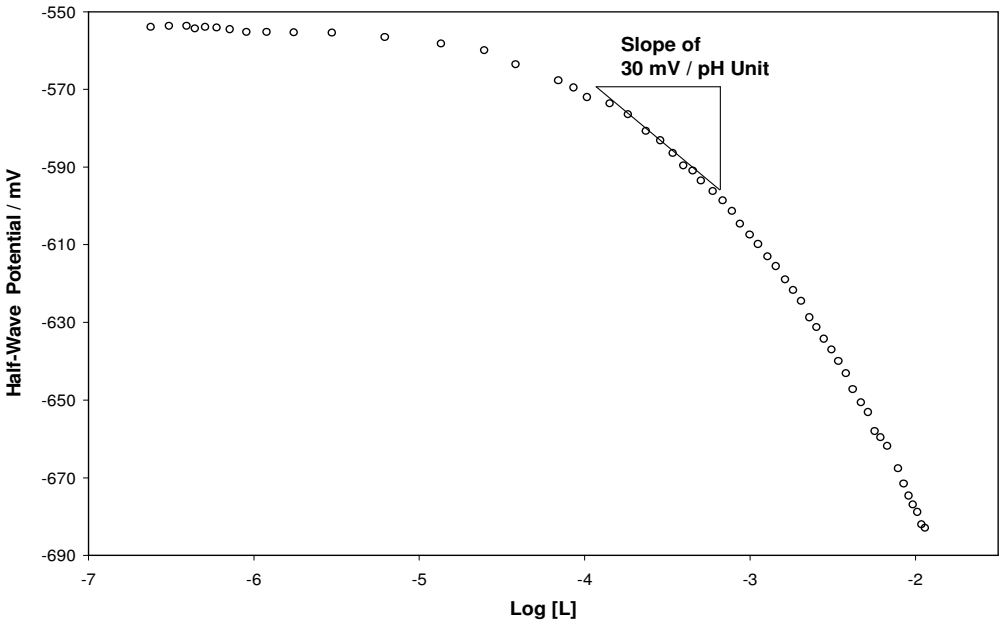


Figure 3.2: An example of a typical relationship of variation in half–wave potential as a function of Log [L].

It follows that the smallest shift one might expect, when this kind of analysis is performed, is about 29–30 mV, when two electrons are involved. This value is a Nernstian slope obtained from $\{q(RT/nF)\}/p$, where q stands for the number of ligands involved in the complex formation reaction and p is set to 1 assuming that

polynuclear species are not formed. Figure 3.2 shows a typical plot of the observed half–wave potential versus the free ligand concentration. The slope that is shown is indicative of formation of an ML complex. This method of predicting species has been applied with success in various polarographic studies of metal–ligand systems [12–14, 18–23].

3.3.2.3 Variation in the limiting diffusion current as a function of pH

A graph of limiting diffusion current as a function of pH usually provides information in support of the proposed model from the predictions made by analyses discussed in preceding sections. If the I(comp) is smaller than the I(M), the decrease in the limiting diffusion current is in a strong support of formation of a metal complex. Typical analysis is done by plotting normalized current, *i.e.*, the ratio I(comp)/I(M), versus pH. If the normalized current does not significantly depart from unity then the system under study can be regarded as fully–labile. Significant decrease in the normalized current would indicate that metal complexes of mixed lability or fully–inert complexes are formed in the pH regions where such decreases are observed [12–14, 18–23].

3.4 VIRTUAL POTENTIOMETRY

A recently developed theory and a concept known as virtual potentiometry (VP) [24–26] was used for further modelling and refinement of polarographic data obtained from metal–ligand equilibria studies. The proposed methodology involves conversion of polarographic data (in the case of DC polarography the relevant data are $I(comp)_{pH(i)}$, $I(M)_{pH(i)}$, and $(E_{1/2}(comp))_{pH(i)}$) into virtual thermodynamic potentials, $E_{1/2}(virt)_{pH(i)}$, calculated from each recorded polarogram at ith pH value. The virtual potentials are calculated according to Equation 3.25. $(E_{1/2}(comp))_{pH(i)}$ is the half–wave potential extracted from the ith polarogram recorded at ith pH step in the presence of metal complexes and $I(\text{comp})_{pH(i)}$ is the corresponding limiting diffusion current; $I(\text{M})_{pH(i)}$ is the limiting diffusion current in the absence of metal complexes.

$$\left(E_{1/2}(\text{comp})\right)_{pH(i)} + \frac{RT}{nF}\ln\left(\frac{I(\text{comp})}{I(\text{M})}\right)_{pH(i)} = E_{1/2}(virt)_{pH(i)} \qquad \textbf{(3.25)}$$

The term I(comp)/I(M) represents the normalized change in the intensity of the recorded polarographic signal. Regardless of the cause of the variation in the intensity of the recorded signal, the term $\{(RT/nF)\ln(I(\text{comp})/I(\text{M}))\}_{\text{pH(i)}}$ can be interpreted as a fraction of a potential by which the recorded polarographic signal should have shifted more towards negative potentials, provided that there was no change in the value of the intensity of the recorded polarographic wave. If the above supposition holds, the theoretically and thermodynamically expected position of the reversible polarographic signal along the potential scale can be written as in Equation 3.25.

There is a well–defined relationship between $E_{1/2}$ and the standard redox potential if the system under investigation can be regarded as thermodynamically fully reversible. For the purpose of this study, *i.e.*, the formation of metal complexes, the redox system considered would be $M^{n+} + ne^- \leftrightarrow M^0$ and the virtual half–wave potential $E_{1/2}$(virt) can be interpreted as a thermodynamic potential of a virtual potentiometric sensor generated from dynamic, nonequilibrium polarographic data. This virtual probe should be sensitive to the change in the free–metal–ion concentration when metal complexes are formed. This virtual potentiometric probe is metal–ion nonspecific and should be able to work for any metal ion that is polarographically active and is reduced reversibly. If all the above holds, the virtual potentiometric sensor should have unlimited linear–response with a theoretical Nernst slope [24–26].

The concept of a virtual potentiometric sensor implies that it should be possible to employ software dedicated for refinement of potentiometric data, such as ESTA, in the refinement of stability constants by using, in principle, data coming from polarography, whereby the refinement operations are exactly the same as those applied for refinement of real potentiometric data.

3.5 ANALYSIS OF DIRECT CURRENT POLAROGRAMS RECORDED ON METAL–LIGAND SYSTEMS

The mathematical methods for treatment of polarographic data described in preceding sections were derived under the assumption that the electrode processes, as measured by a particular polarographic technique, are reversible and polarographic signals analysed must contain information due to reduction of a labile species in homogeneous equilibrium with other species in solution. Furthermore, the mathematical methods are also applicable if the degree of reversibility corresponding to all recorded polarograms does not vary throughout the entire experiment [11, 24–26]. Consequently, recorded polarographic curves have to be analyzed as accurately as possible, (i) to establish electrochemical reversibility, and (ii) if there is departure from electrochemical reversibility, to obtain, if possible, the reversible half–wave potential and the limiting diffusion current values from the recorded polarograms at various pH values.

3.5.1 Electrochemical Reversibility: General Concepts

In its most general form, an electrode process consists of a charge or electron transfer step (heterogeneous kinetics), the chemical reactions coupled to that charge transfer step (homogeneous kinetics), and diffusion. The measured response for an overall electrode process, as measured by a particular technique, will then reflect both heterogeneous and homogeneous kinetics. An electrode process occurring across a solution–electrode interface can loose its reversible character because of either a slow electron transfer step (slow heterogeneous kinetics) or a slow chemical step associated to the overall electrochemical process (slow homogeneous kinetics), and a given polarographic technique can respond to an electrode process in a decidedly different fashion depending on the cause of the non–reversibility or kinetic complication. It follows that, in each polarographic technique, the question of reversibility needs to be defined explicitly within the realms of its own time domain [27]. In general, when the time available for establishing equilibrium is shortened, then the electrode process under consideration looses its reversible character [28].

It should be noted that electrode processes that depart from reversibility (dealt in this discussion and in the project as whole) will be those that are due to slow heterogeneous kinetics, with the assumption of fast homogeneous kinetics relative to the timescale of DC polarography.

In polarography, a given polarogram is the result of an electrode process occurring when a potential is applied to a cell and the resulting current–potential curve is generally amenable to a kinetic description. The application of a potential, as in a polarographic experiment, necessarily perturbs the system under study. If the various kinetic processes associated with the overall electrode process are sufficiently fast, or the perturbation is applied sufficiently slowly, the system can maintain its equilibrium state within the limit of experimental error of the measuring method employed to follow the system [28]. An electrode process is described as reversible if the equilibrium between the oxidized and reduced forms is established so rapidly that the electrode potential can be described by Nernst equation and the current is controlled only by the rate of diffusion of the electroactive species to the dropping mercury electrode [29].

Any process is of course only strictly *thermodynamically reversible* when an infinitesimal change in the direction of a driving force causes the direction of the process to reverse. All electrode processes and reactions occur at a finite rate and therefore do not proceed with thermodynamic reversibility. Thus, a *practical definition of reversibility* is really being used in defining a reversible electrode process as one obeying the Nernst equation, the implication being that departures from thermodynamic reversibility are too small to measure with the particular technique under consideration. The most general and useful descriptions of an electrode process are therefore formulated in terms of kinetic equations and the conditions, e.g., rate constants, required for practical reversibility noted. Electrode processes that do not meet the specified conditions for reversibility can then be said to be non–reversible or non–Nernstian [27].

Consider the electrochemical reduction of a complexed ion ML_j, that is predominant in solution, to the metallic state (as an amalgam) at the dropping mercury electrode. The overall electrode reaction may be expressed as:

$$ML_j + ne + Hg \leftrightarrow M(Hg) + jL$$

For convenience, this overall process may be represented as being made up of two reactions, the first involving prior dissociation of the complex ion into metal complexes of lower coordination number and the aquo metal ion with liberation of ligand molecules (homogenous kinetics), the second being the actual electrochemical reaction of the electroactive species, which may be a metal complex of lower coordination number than ML_j or the aquo metal ion (heterogeneous kinetics). This situation is presented in the scheme below:

$$\underbrace{ML_j(aq) \leftrightarrow ML_{j-1} + L \leftrightarrow \ldots \leftrightarrow M(aq) + jL(aq)}_{\text{Homogenous kinetics}}$$

$$\Updownarrow ne,\ k_s \quad \text{Heterogeneous kinetics}$$

$$M(Hg) + jL$$

In the scheme above, k_s denotes the heterogeneous rate constant for the overall electrochemical process at standard potential E°.

The reversibility of the polarogram that will be recorded for the above reduction process (assuming fast homogeneous kinetics) is determined by the energetics involved in the overall heterogeneous electron transfer process, which would be controlled by the magnitude of k_s [29].

For practical classification of degree of reversibility of electrode processes, the magnitude of k_s is used. In general, large values of k_s correspond to very fast electron transfer processes (fast heterogeneous kinetics) and small values of k_s correspond to non–reversible processes. As noted above, any discussion of electrochemical reversibility has to be with respect to the measuring technique used and the relevant time domain applied. The time domain of a DC polarographic experiment is governed by the drop time, so that the value of k_s

required to define a reversible electron transfer step needs to be stated with respect to a specific drop time. Delahay [30] showed that if $k_s \geq 2 \times 10^{-2}$ cm s^{-1}, a DC electrode process can be considered reversible for a drop time of approximately 3 seconds. If k_s lies within the limits $2 \times 10^{-2} \geq k_s \geq 5 \times 10^{-5}$ cm s^{-1}, DC polarographic curves are classified as quasi–reversible and for a totally irreversible electrode process $k_s \leq 5 \times 10^{-5}$ cm s^{-1}.

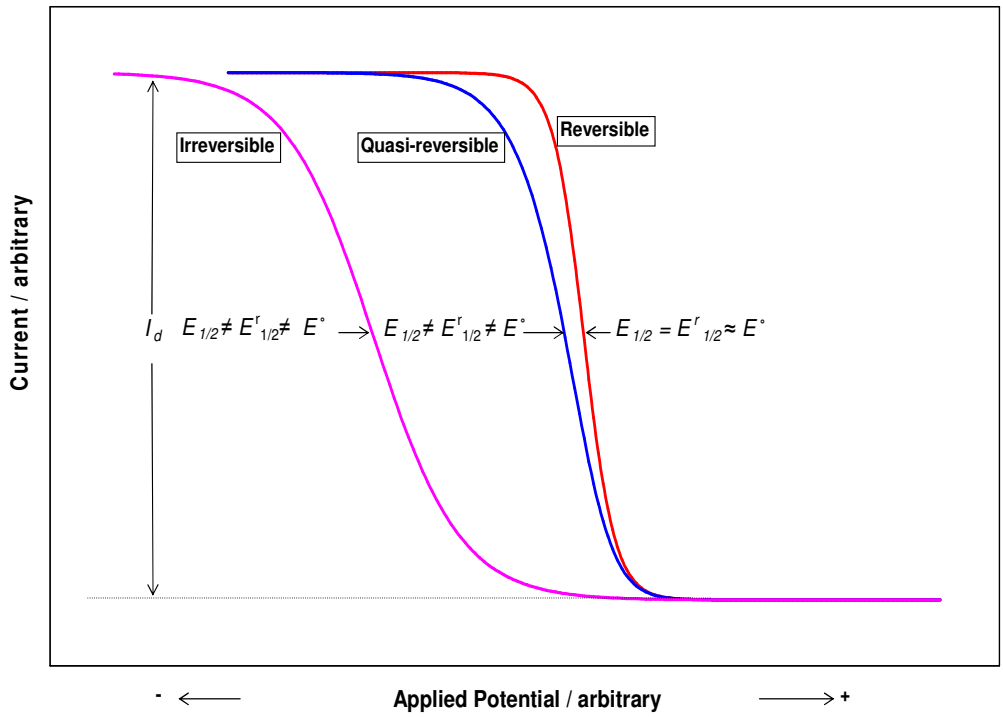


Figure 3.3: Schematic comparison of DC polarograms corresponding to reversible, quasi–reversible, and irreversible reduction processes. $E_{1/2}$ and $E^r_{1/2}$ stand for observed half–wave potential and reversible half–wave potential, respectively. E° stands for the standard reduction potential.

In general, a reversible electrode process can also be defined as one in which diffusion control rather than the electron transfer step is the determining factor. This class of electrode process is characterized by large values of k_s, and the current magnitude at all potentials is considered to be independent of k_s within the limit of experimental error of the method of measurement. If the electrode process

is controlled by kinetics of the electron transfer step as well as diffusion, then a non–reversible electrode process results [27]. A comparison of the shapes of typical DC polarographic curves for a reversible, quasi–reversible and totally irreversible reduction processes is given in Figure 3.3.

In DC polarography if the electrode process is reversible, the observed half-wave potential $E_{1/2}$ (which is coincident with the reversible half–wave potential $E^{r}_{1/2}$) occurs at a potential very near the standard potential ($E°$) for the redox couple involved. Hence, reversible half–wave potentials are used in determining thermodynamic parameters such as stability constants, Gibbs free energy etc. It is evident in Figure 3.3, that the limiting diffusion current (I_d) is the same for the polarograms shown. This is a unique feature of DC polarography, i.e., the limiting diffusion current remains essentially the same regardless of the degree of reversibility. This feature holds for an electrode process that involves the same number of electrons and is determined with the same capillary and solution characteristics [27].

In the case of the reversible wave, the current is controlled at all times by the rate of diffusion of the electroactive species to the dropping mercury electrode (DME), the electron transfer occurring very rapidly. Over a large part of the irreversible wave the rate, and therefore the current, is controlled mainly by the electrode reaction rate. As the applied potential is increased the rate of the electrode reaction increases and at sufficiently negative potentials may be comparable with the diffusion rate. As the applied potential is increased even further to considerably more negative potentials, the electrode reaction occurs very rapidly in comparison with the diffusion process, which becomes rate-determining. It is for this reason that I_d is essentially the same for reversible or non–reversible waves [28].

3.5.2 Evaluation of Electrochemical Reversibility

3.5.2.1 Logarithmic analysis

The classical method for evaluation of electrochemical reversibility from analysis of a DC polarogram involves what is termed *logarithmic analysis*, which is a graphical procedure that derives from the Ilkovič–Heyrovský equation (Equation 3.26), an equation that describes the current–potential relationship of a reversible reduction process occurring at the DME [28, 29,31].

$$I_{\text{red}} = \frac{I_{\text{d}}}{\exp \frac{nF}{RT}(E_{\text{appl}} - E_{1/2}) + 1} \qquad \textbf{(3.26)}$$

Equation 3.26 can be rearranged in a logarithmic form as:

$$\text{Log}\left(\frac{I_{\text{red}}}{I_{\text{d}} - I_{\text{red}}}\right) = \frac{nF}{2.303\ RT} E_{1/2} - \frac{nF}{2.303\ RT} E_{\text{appl}} \qquad \textbf{(3.27)}$$

In Equations 3.26 and 3.27, I_{red} stands for the reduction current developed from the reduction processes at the dropping mercury electrode; I_{d} is the limiting diffusion current; E_{appl} is the stepwise applied potential at which the current was recorded; $E_{1/2}$ is the observed half–wave potential; n is the number of electrons involved in the overall reduction process at the DME; F, R, and T have their usual meanings in physical chemistry.

It is evident from Equation 3.27 that, for a reversible reduction process, a graphical plot of Log ($I_{\text{red}}/I_{\text{d}} - I_{\text{red}}$) versus $-E_{\text{appl}}$ should be a straight line with intercept (on the E_{appl} axis) equal to $E_{1/2}$ and slope of $\{nF/2.303RT\}$. This follows from the fact that $E_{\text{appl}} = E_{1/2}$ at Log ($I_{\text{d}} - I_{\text{red}}/I_{\text{red}}$) = 0 and Log ($I_{\text{d}} - I_{\text{red}}/I_{\text{red}}$) = 0 if and only if $I_{\text{red}} = I_{\text{d}}/2$, the latter situation holds when $E_{\text{appl}} = E_{1/2}$. Moreover, if the reduction process is reversible, the observed $E_{1/2}$ is coincident with the reversible half–wave potential ($E^{r}_{1/2}$).

It must be noted that any logarithmic analysis of a DC polarogram requires evaluation of I_d prior to performing the analysis to test for electrochemical reversibility. Furthermore, background current has to be accounted for and subtracted from the observed total current before a logarithmic analysis can be performed.

Although Equation 3.26 is an important polarographic relationship, as a criterion of reversibility it should be used with great caution. A linear plot is very often obtained for processes classed as irreversible although the slope obtained would significantly differ from the reversible slope [27]. This situation arises because for irreversible processes in DC polarography, the current–potential relationship is described by an extended Ilkovič–Heyrovský equation given below:

$$I_{red} = \frac{I_d}{\exp \frac{\alpha nF}{RT}(E_{appl} - E_{1/2}) + 1} \quad \textbf{(3.28)}$$

The corresponding logarithmic form of Equation 3.28 is given as:

$$\text{Log}\left(\frac{I_{red}}{I_d - I_{red}}\right) = \frac{\alpha nF}{2.303\ RT}E_{1/2} - \frac{\alpha nF}{2.303\ RT}E_{appl} \quad \textbf{(3.29)}$$

In Equations 3.28 and 3.29, α is the cathodic transfer coefficient, a dimensionless parameter that may be regarded as fraction of the applied potential which either assists or hinders the reduction process under consideration. It is practically a measure of the symmetry of the energy barrier for an electron transfer process. Also, for the faradaic current, I_{red}, corresponding to the reduction process in this case, is no longer the diffusion–controlled value but is governed by the electron transfer rate. However, the limiting current I_d is still the diffusion–controlled value. Furthermore, $E_{1/2}$ of an irreversible polarogram is not coincident with the reversible half–wave potential [29].

It is obvious from Equation 3.29 that a plot of Log ($I_{red}/I_d - I_{red}$) versus $-E_{appl}$, corresponding to an irreversible electrochemical process in DC polarography, should also be linear with slope of about $\{\alpha nF/2.303RT\}$.

Since one would typically be dealing with known metal ions, e.g., Zn^{2+}, Pb^{2+}, or Cd^{2+}, and hence, the number of electrons n involved in the electrochemical process at the DME would be known, then a better test of reversibility to distinguish between a reversible and irreversible polarogram, from a logarithmic analysis, is to calculate n using the slope observed from the logarithmic plot [27]. In this regard, one equates the observed slope to the theoretical slope, as given in Equation 3.27, to calculate n. The theoretical slope presented in Equation 3.27 can be simplified as follows:

$$\frac{nF}{2.303\,RT} = \frac{n}{\frac{2.303\,RT}{F}} = \left(\frac{n}{0.05916}\right) \text{Volts} \qquad \text{(at 25 °C)} \qquad \textbf{(3.30)}$$

Therefore, at 25 °C,

$$\boldsymbol{n} = \textbf{(Observed slope from logarithmic plot)} \times \textbf{0.05916} \qquad \textbf{(3.31)}$$

For a reversible polarogram, the calculated value of n should be close to the true value of n (For Cd^{2+} or Pb^{2+} the true value of n would be 2). If the calculated value of n, using Equation 3.32, is significantly different from the true value of n, then one concludes the polarogram analyzed corresponds to an irreversible process.

A typical DC polarogram corresponding to a reversible reduction process is shown in Figure 3.4. The corresponding logarithmic analysis is shown in Figure 3.5. The procedure used for fitting the polarogram in Figure 3.4 is described at a later discussion in this chapter (section 3.5.3).

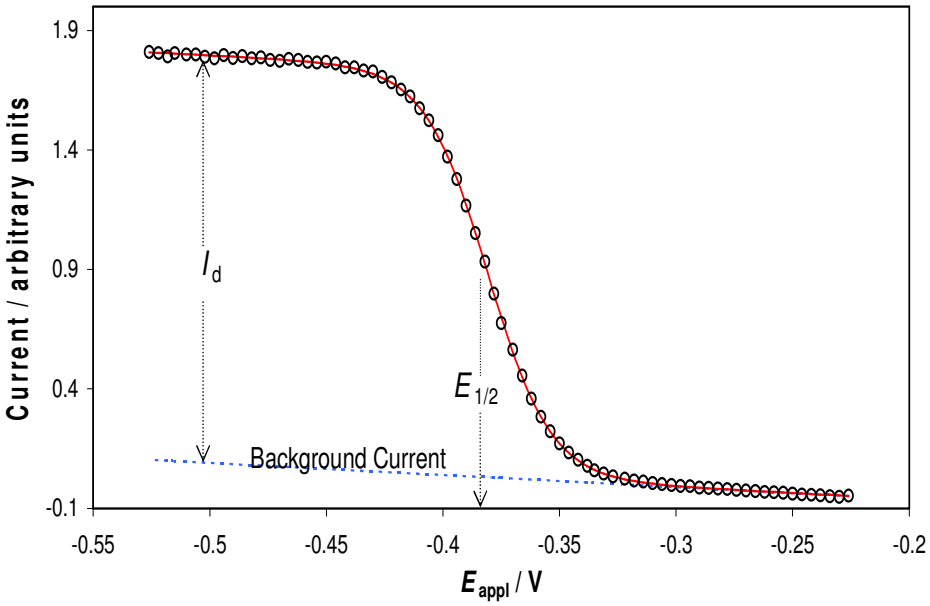


Figure 3.4: A sampled direct current polarogram for the reversible reduction of Pb^{2+} at 25 °C in 0.5 M $NaNO_3$. Circles indicate the experimental points while solid line is fitted to estimate the limiting diffusion current (I_d).

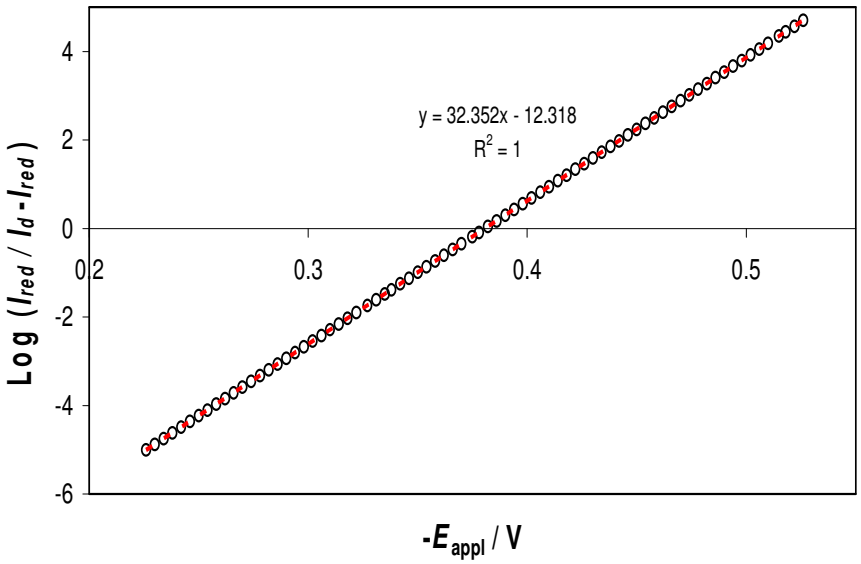


Figure 3.5: A logarithmic analysis corresponding to the DC polarogram for the reversible reduction of Pb^{2+} at 25 °C in 0.5 M $NaNO_3$ shown in Figure 3.4. Circles indicate the experimental points while the dashed line is a fitted linear trendline. See text for interpretation details.

From the observed slope of the logarithmic plot shown in Figure 3.5, and using Equation 3.32, $n = 32.352 \times 0.05916 = 1.91 \approx 2$. The calculated value of n clearly indicates that the DC polarographic reduction process for Pb^{2+}, in this case, is fully–reversible.

At this point of this discussion one is prompted to ask how to evaluate electrochemical reversibility from quasi–reversible polarograms by performing logarithmic analysis. The answer is, no simple solution is available as was the case for reversible and irreversible polarograms discussed above. In general, for quasi–reversible polarograms, a plot of Log $(I_{red}/I_d - I_{red})$ versus $-E_{appl}$ is curved [27]. An example of a quasi–reversible polarogram and its corresponding logarithmic analysis are given in Figures 3.6 and 3.7.

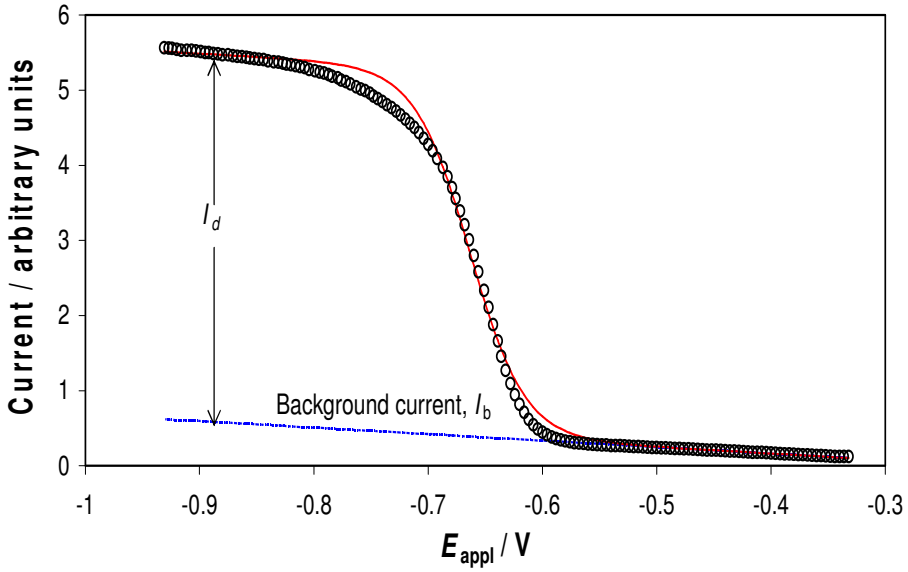


Figure 3.6: A sampled direct current polarogram for a quasi–reversible reduction of Cd^{2+} at 25 °C in 0.5 M $NaNO_3$ in the presence of the ligand sarcosine. Circles indicate the experimental points while solid line is fitted to estimate the limiting diffusion current (I_d).

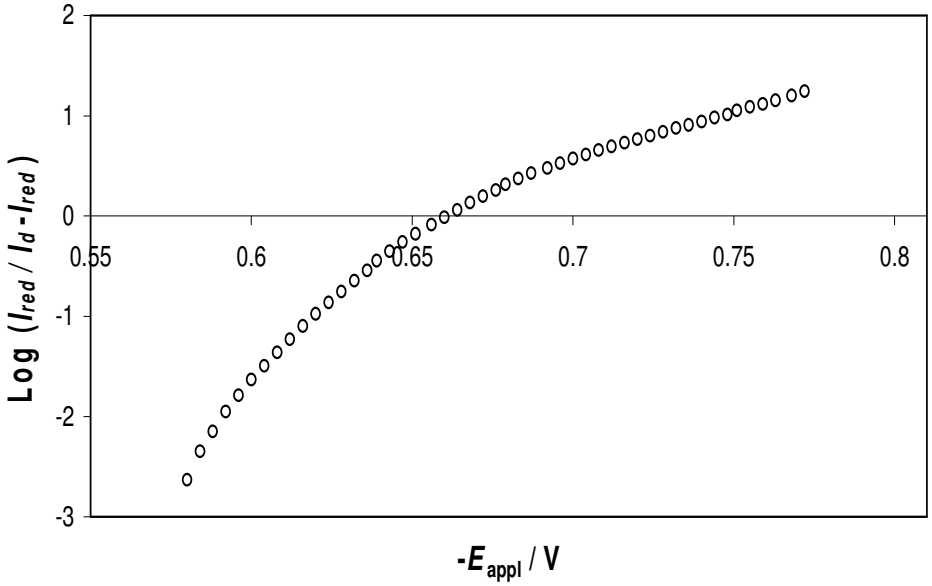


Figure 3.7: A logarithmic analysis of the DC polarogram seen in Figure 3.6. The curved logarithmic plot indicates a quasi–reversible reduction process.

Construction of a large number of logarithmic plots from DC polarograms for purposes of evaluating electrochemical reversibility is a tedious and time–consuming procedure. An expedient alternative procedure is to employ a curve–fitting procedure whereby a whole DC polarogram is analyzed by fitting a function to the experimental data using an appropriate curve–fitting computer program.

3.5.2.2 Curve–fitting method

A simple nonlinear curve–fitting method (Equation 3.32) for analysis of DC polarograms for purposes of evaluating electrochemical reversibility has been proposed by Cukrowski [24–25]. The equation used is essentially that already encountered in this discussion, namely, the equation describing the current–potential relationship of an irreversible DC polarogram (see Equation 3.28). In this case, the coefficient α in the equation for an irreversible DC polarogram is replaced with another coefficient, namely δ. The coefficient δ has no physical meaning as the transfer coefficient α, but as a parameter in curve–fitting it

describes how steep the polarographic wave is, and thus the coefficient δ is used for evaluating electrochemical reversibility of DC curves.

The parameter δ should be equal to 1 for fully reversible systems. For all practical purposes δ values above 0.9 indicate reversible systems, and δ values below 0.9 indicate non–reversibility. Typically, δ values between 0.5 – 0.9 suggest quasi–reversible systems. δ values of about 0.5 and below would then suggest irreversible systems.

$$I_{\text{red}} = \frac{I_{\text{d}}}{\exp\frac{\delta nF}{RT}(E_{\text{appl}} - E_{1/2}) + 1} \qquad \textbf{(3.32)}^{2}$$

It should be noted that Equation 3.32 can only be used directly in nonlinear curve–fitting of a DC polarogram if and only if background current in such a polarogram is accounted for prior to the fitting operation. Since background current in voltammetry generally depend on E_{appl}, an appropriate function is added to Equation 3.32 to account for it. A linear function is usually sufficient to account for background current. A complete model to be used directly in curve–fitting of a DC polarogram is then compiled as:

$$I_{\text{obs}} = \frac{I_{\text{d}}}{\exp\frac{\delta nF}{RT}(E_{\text{appl}} - E_{1/2}) + 1} + I_{\text{b}} \qquad \textbf{(3.33)}^{3}$$

In Equations 3.32 and 3.33, I_{red}, I_{b}, and I_{obs} stand for the reduction, background and observed total current; n stand for number of electrons (for Cd^{2+}, Pb^{2+}, and Zn^{2+} n = 2), E_{appl} is the stepwise applied potential (in Volts) at which the total current was recorded, I_{d} is the limiting diffusion current, $E_{1/2}$ is the half–wave

[2] For curve–fitting of DC polarograms recorded at 25 °C, as in the original publications, this equation can be implemented as:

$$I_{\text{red}} = \frac{I_{\text{d}}}{10^{\frac{\delta nF}{2.303\,RT}(E_{\text{appl}} - E_{1/2})} + 1} = \frac{I_{\text{d}}}{10^{((\delta n(E_{\text{appl}} - E_{1/2}))/0.05916)} + 1}$$

The constant $F/2.303RT$ = 1/0.05916 V at 25 °C.

[3] This curve-fitting model will also be referred to as the **Cukrowski's curve–fitting method**.

potential and δ is the steepness coefficient (or reversibility index); F, R, and T have their usual meaning.

The unknown parameters in the model given by Equation 3.33 are: δ, $E_{1/2}$, I_d, and constants in the function I_b describing the background current. In this project, for the metal–ligand systems studied, I_b was given as:

$$I_b = a + bE_{appl} \quad \textbf{(3.34)}$$

or

$$I_b = a + bE_{appl} + c\exp(-dE_{appl}) \quad \textbf{(3.35)}$$

For metal–ligand systems involving Cd^{2+} and Pb^{2+}, Equation 3.34 was used to account for background current in the nonlinear curve-fitting operations. For metal–ligand systems involving Zn^{2+}, I_b was given either as Equation 3.34 or Equation 3.35 depending on the pH range at which the polarograms were recorded. The exponential term was added to account for hydrogen evolution that contributed to the background current in some pH ranges. Thus, the unknown variables for the background term would be a and b, or a, b, c, and d. Since all experiments in this project were conducted at 25 °C and $n = 2$ for the metal ions studied (Cd^{2+}, Pb^{2+}, Zn^{2+}), the parameters n, F, R, and T are known (nF/RT = 77.848 V for $n = 2$, $T = 25$ °C).

The Curve–fitting Algorithm

In all curve–fitting operations performed in this project, a Marquardt–Levenberg algorithm [32] was adopted. A computer program *Precision Curve Fitter* [33] was used in this regard. The basis of the nonlinear curve–fitting algorithm is well known. In summary, the computer programs for nonlinear regression begin with a set of best guesses for the parameters in the model, as provided by the user. Matrix manipulations within the computer progressively improve those parameters values by minimizing the objective function given in Equation 3.36:

$$\sum_{j=1} (I_{\text{obs}} - I_{\text{calc}})^2_{E_j} \qquad \textbf{(3.36)}$$

where E_1, E_2,…, E_j are the stepwise applied potentials at which the total observed current I_{obs} for the polarogram was recorded; I_{calc} is the corresponding calculated current value from the regression equation using the parameters that are varied.

After a sufficient number of iterations no significant further improvement occurs and the latest batch of parameters is taken as final, i.e., convergence takes place.

3.5.3 Determination of Reversible Half–Wave Potential and Limiting Diffusion Current

A polarographic experiment of a metal–ligand system would generate a set of polarograms that would first be checked to ascertain the degree of reversibility and decide on the most appropriate method of analysis to extract the required parameters (I_d and $E_{1/2}$) for subsequent use in modelling and determination of stability constants.

As mentioned in the introductory chapter, one of the aims of this project was to investigate feasibility of using selected theoretical equations from the literature to develop nonlinear curve–fitting models. They were to be used in computer–based curve–fitting procedures for fast and reliable prediction of reversible half–wave potential values from DC polarograms that are recorded in polarographic studies of metal–ligand equilibria and which exhibit departure from reversibility.

3.5.3.1 Reversible or nearly reversible systems

Direct current polarograms that are evaluated to be reversible using the criteria described in section 3.5.2 (for example, δ values above 0.9) are relatively simple to analyse by performing nonlinear regression analysis on them. The model used is the same as that already described in section 3.5.2, i.e., the Cukrowski's curve–fitting method (Equation 3.33). The fitted parameters I_d and $E_{1/2}$, associated with

the best–fit, would then correspond to the limiting diffusion current and reversible half–wave potential required for subsequent modelling and refinement operations with the final aim of determining stability constants for the metal–ligand system under consideration.

3.5.3.2 Non–reversible systems

(i) *Nonlinear Curve-fitting of Quasi–Reversible Polarograms using the Cukrowski's curve–fitting method*

For analysis of quasi–reversible DC polarograms with slight departures from reversibility, the Cukrowski's curve–fitting method (Equation 3.33) described in previous section has also been shown to be useful, as a nonlinear curve–fitting model, for estimating reversible half–wave potentials [24]. Figure 3.8 shows a quasi–reversible DC polarogram fitted using this method.

The model is implemented in, a stepwise fashion, as follows:

- All experimental points of the DC polarogram are fitted using Equation 3.33 to obtain the parameters I_d, $E_{1/2}$, δ, and parameters of the function estimating background current, I_b (for example, if $I_b = a + bE_{appl}$, these parameters would be a and b).
- A set of experimental points (starting at E_{appl} value corresponding to about one–fifth of the I_d and ending at an E_{appl} value in the limiting region) are disallowed. In Figure 3.8, the disallowed points are presented as circles with solid dots.
- Then, a second curve–fitting operation is performed with the parameter δ kept fixed at the value of 1 (this is tantamount to forcing full electrochemical reversibility). Also, the parameter I_d is fixed at the value obtained from the first curve–fitting operation (fixing I_d at this value is valid as I_d does not depend on the degree of reversibility in DC polarography). The $E_{1/2}$ value obtained is then regarded as the reversible half–wave potential ($E^r_{1/2}$).

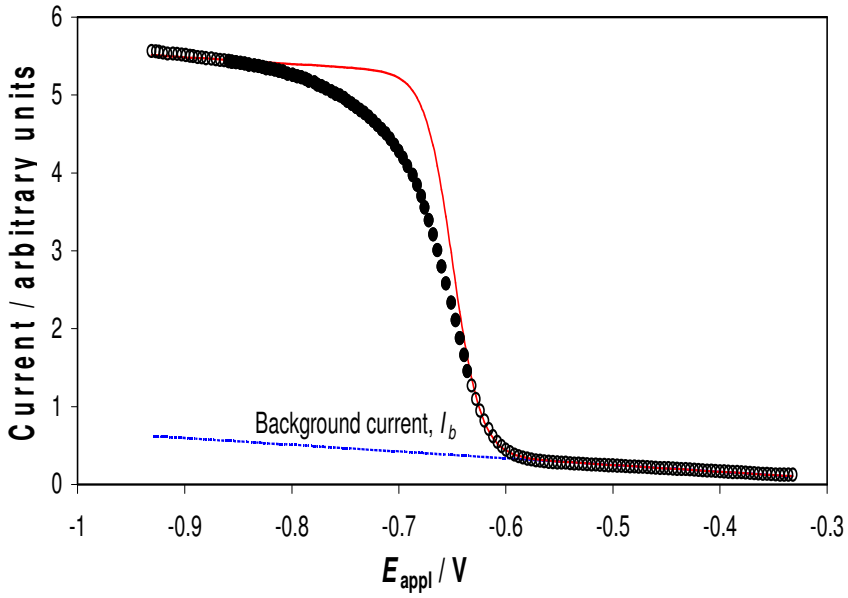


Figure 3.8: An example of the analysis of a quasi–reversible DC polarogram for the reduction of Cd^{2+} at 25 °C in 0.5 M $NaNO_3$, in the presence of the ligand sarcosine, using the Cukrowski's curve–fitting method. Open circles (o) represent recorded experimental points; the solid line represents the computed DC polarogram obtained from the curve-fitting operation (see text for details).

(ii) *Nonlinear Curve–fitting of Non–Reversible Polarograms using a model derived from Matsuda–Ayabe method*

For the quasi–reversible DC polarographic waves resulting from reduction of metal ions either in complexed form or as free metal ions, Matsuda and Ayabe [34–37] derived the following equation to describe the current–potential relationship:

$$I_{\text{red}} = \frac{I_{\text{d}}}{1.13\,(\Lambda\sqrt{\tau})^{-1}\exp\frac{\alpha nF}{RT}(E_{\text{appl}} - E^{r}_{1/2}) + \exp\frac{nF}{RT}(E_{\text{appl}} - E^{r}_{1/2}) + 1} \qquad \textbf{(3.37)}$$

In logarithmic form Equation 3.37 is given as:

$$\mathrm{Log}\left(\frac{I_{\mathrm{red}}}{I_{\mathrm{d}}-I_{\mathrm{red}}}\right)=\mathrm{Log}\left(1.13(\Lambda\sqrt{\tau})^{-1}\exp\frac{\alpha nF}{RT}(E_{\mathrm{appl}}-E^{r}_{1/2})+\exp\frac{nF}{RT}(E_{\mathrm{appl}}-E^{r}_{1/2})\right) \quad \textbf{(3.38)}$$

where

$$I_{\mathrm{d}}=(24/7)(7\pi/3)^{\frac{1}{2}}(3/4\pi d)^{\frac{2}{3}}nFD_{\mathrm{j}}^{\frac{1}{2}}C_{\mathrm{j}}m^{\frac{2}{3}}\tau^{\frac{1}{6}} \text{ (Ilkovič Equation)} \quad \textbf{(3.39)}$$

(j = ox, for the reduction of free metal ions, and j = *N*, for the reduction of complex ions)

$$\Lambda=k_{\mathrm{s}}\left(f_{\mathrm{ox}}/D_{\mathrm{ox}}^{1/2}\right)^{1-\alpha}\left(f_{\mathrm{red}}/D_{\mathrm{red}}^{1/2}\right)^{\alpha} \quad \textbf{(3.40)}$$

for reduction of free metal ions, or

$$\Lambda=(k_{\mathrm{s}})_{\mathrm{B}}\left(f_{\mathrm{N}}/D_{\mathrm{N}}^{1/2}\right)^{\beta}\left(f_{\mathrm{red}}/D_{\mathrm{red}}^{1/2}\right)^{\alpha}(f_{\mathrm{x}}C_{\mathrm{x}})^{-\beta N+p} \quad \textbf{(3.41)}$$

for the reduction of complex ions.

$E^{r}_{1/2}$ *is* the reversible half–wave potential; τ is the mercury drop life time employed during the DC polarographic scan; *d* is the specific density of mercury; k_{s} and $(k_{\mathrm{s}})_{\mathrm{B}}$ are heterogeneous rate constants for the electrode processes involving a simple metal ion and overall reduction of a complexed metal ion, respectively; α and β are the cathodic and anodic transfer coefficients such that $\alpha + \beta = 1$; C_j and C_x are the concentrations of the oxidized form of the species predominant in solution, and of the free ligand, respectively; f_{j}, f_{red}, f_{x} are the corresponding activity coefficients (the activity coefficients can practically be considered equal to 1 at constant ionic strength and for very dilute solutions); D_{j} and D_{red}, are the corresponding diffusion coefficients; *N* and *p* are the numbers of ligands in the predominant complex in solution and the electroactive complex, respectively.

The implicit assumptions in the derivation of the Matsuda–Ayabe equation above are summarized below:

- The overall electrode process resulting in a given polarogram is controlled by the electrode kinetics and/or linear diffusion, i.e., current at any given

point is either controlled by the rate of electrode process (heterogeneous kinetics) and/or by the rate of diffusion of the species reacting at the DME. Furthermore, the limiting current is diffusion–controlled.

- The electrode kinetics follows Butler–Volmer type of kinetics, whereby $\alpha + \beta = 1$, and α is independent of applied potential.
- Reduction of a complexed ion ML_N that is predominant in solution, proceed via intermediates of lower coordination number, whereby there is a labile equilibrium (fast homogeneous kinetics) between the predominant complexed ion and the actual species that is electrochemically reduced ML_p (p = 0, .., N, if p = 0, then ML_p is simply the free metal ion M). The overall reaction

$$ML_N + ne + Hg \leftrightarrow M(Hg) + NL$$

can be considered as separated into a series of reactions. The assumption is that the overall reaction follows the following sequence: Complex ML_N, which is the major component in solution, diffuses to the surface of the electrode and from there it dissociates stepwise into the electroactive species ML_p. The produced species ML_p participates in the electrochemical reduction process:

$$ML_N \leftrightarrow ML_{N-1} + L \leftrightarrow \ldots \leftrightarrow ML_p + ne + Hg \leftrightarrow M(Hg) + NL$$

For the determination of the transfer coefficient α and reversible half–wave potential $E^r_{1/2}$, Matsuda and Ayabe performed a logarithmic analysis, i.e., a plot of Log $(I_{red}/I_d - I_{red})$ versus $-E_{appl}$, which for a quasi–reversible DC polarogram would be curved. For illustrative purposes such a plot is presented in Figure 3.9. From the logarithmic plot α is determined from the slope of a straight line tangent to the curve at sufficiently negative potentials:

$$\alpha = 2.3(RT/nF)\left\{\frac{\Delta \mathrm{Log}\,[I_{red}/(I_d - I_{red})]}{\Delta(-E_{appl})}\right\} \qquad \textbf{(3.42)}$$

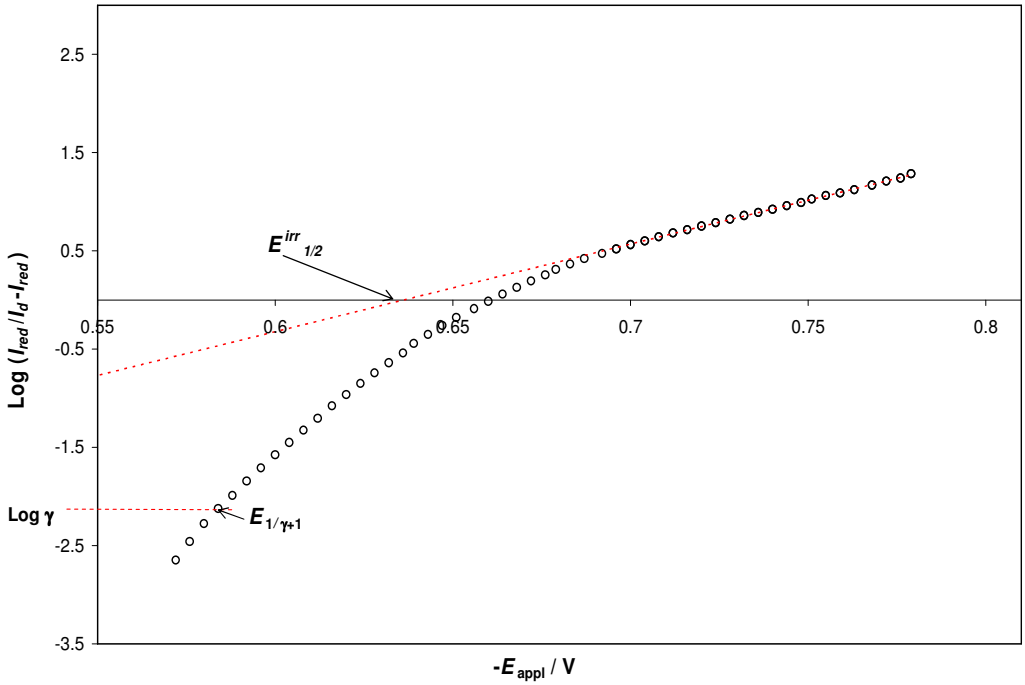


Figure 3.9: Logarithmic analysis of a quasi–reversible DC polarographic wave using the Matsuda–Ayabe method (see text for details).

In order to determine $E^{r}_{1/2}$ with the Matsuda–Ayabe method, two potentials $E^{irr}_{1/2}$ and $E_{1/\gamma+1}$ are chosen, where γ is some ($I_{red}/I_d - I_{red}$) ratio at the foot of the polarographic wave and $E_{1/\gamma+1}$ is the corresponding potential (see Figure 3.9 for illustration). From the potentials $E^{irr}_{1/2}$ and $E_{1/\gamma+1}$, and α as determined by Equation 3.42, $E^{r}_{1/2}$ is found using the following equation:

$$E^{r}_{1/2} = E_{1/\gamma+1} - 2.3(RT/nF)\left\{\text{Log}[\gamma - \exp(\alpha nF/RT\,(E_{1/\gamma+1} - E^{irr}_{1/2})\right\} \qquad \textbf{(3.43)}$$

The proposed curve–fitting model based on Matsuda–Ayabe Equation

The proposed nonlinear curve–fitting model in this project, for analysis of non–reversible DC polarograms based on the Matsuda–Ayabe equation (Equation 3.37), is given below:

$$I_{\text{obs}} = \frac{I_{\text{d}}}{\Gamma \exp \frac{\alpha nF}{RT}(E_{\text{appl}} - E^{r}_{1/2}) + \exp \frac{nF}{RT}(E_{\text{appl}} - E^{r}_{1/2}) + 1} + I_{\text{b}} \qquad \textbf{(3.44)}$$

where

$\Gamma = 1.13(\Lambda\sqrt{\tau})^{-1}$; Λ is the kinetic parameter as given by Equations 3.40 or 3.41; τ is the mercury drop life time employed during the DC polarographic scan; I_{obs} stands for the observed total current, n stands for number of electrons, E_{appl} is the stepwise applied potential (in volts) at which the total current was recorded, α is the cathodic transfer coefficient; I_{b} is a function describing the background current; $E^{r}_{1/2}$ is the reversible half–wave potential; and I_{d} is the limiting diffusion current; *n, F*, *R*, *and T* have their usual meanings.

The model given by Equation 3.44 was derived from the Matsuda–Ayabe equation (Equation 3.37) by considering the term $1.13(\Lambda\sqrt{\tau})^{-1}$ as an unknown constant parameter Γ. Hence, the model has the following unknown parameters: α, I_{d}, $E^{r}_{1/2}$, Γ and parameters of the function I_{b} describing background current. In a nonlinear curve–fitting operation, these parameters would be varied to try to reproduce a non–reversible DC polarogram with the aim of predicting the reversible half–wave potential $E^{r}_{1/2}$.

(iii) *Nonlinear Curve-fitting of Non–Reversible Polarograms using a model based on Ružić Equation*

Another method for analysis of quasi–reversible DC polarographic waves found in literature is that derived by Ružić and co-workers [38]. Ružić and his co-workers derived their method from the Matsuda–Ayabe method mentioned in the preceding section. Ružić and co–workers found that:

$$1.13(\Lambda\sqrt{\tau})^{-1} \exp \frac{\alpha nF}{RT}(E_{\text{appl}} - E^{r}_{1/2}) = \exp \frac{\alpha nF}{RT}(E_{\text{appl}} - E^{irr}_{1/2}) \qquad \textbf{(3.45)}$$

and the equation derived is given as:

$$\mathrm{Log}\left(\frac{I_{\mathrm{red}}}{I_{\mathrm{d}} - I_{\mathrm{red}}}\right) = \mathrm{Log}\left(\exp\tfrac{nF}{RT}(E_{\mathrm{appl}} - E^{r}_{1/2}) + \exp\tfrac{\alpha nF}{RT}(E_{\mathrm{appl}} - E^{irr}_{1/2})\right) \qquad \textbf{(3.46)}$$

Ružić and co–workers determined $E^{r}_{1/2}$ and α graphically from logarithmic analysis derived from Equation 3.46.

In Equation 3.46, I_{red} is the reduction current; I_{d} is the limiting diffusion current; E_{appl} is the stepwise applied potential at which the total current was recorded; α is the cathodic transfer coefficient; $E^{r}_{1/2}$ is the reversible half–wave potential; $E^{irr}_{1/2}$ is the 'irreversible' half–wave potential corresponding to the irreversible part of the DC wave ($E^{irr}_{1/2}$ is not equal to observed half–wave potential $E_{1/2}$ as recorded from a DC polarogram); n, F, R, and T have their usual meanings.

The proposed curve–fitting model based on the Ružić equation

Rearranging the logarithmic form of the Ružić equation (Equation 3.46), to express the reduction current I_{red} as an explicit function of the applied potential E_{appl} one obtains:

$$I_{\mathrm{red}} = \frac{I_{\mathrm{d}}}{\exp\tfrac{\alpha nF}{RT}(E_{\mathrm{appl}} - E^{irr}_{1/2}) + \exp\tfrac{nF}{RT}(E_{\mathrm{appl}} - E^{r}_{1/2}) + 1} \qquad \textbf{(3.48)}$$

The proposed nonlinear curve–fitting model in this project, for analysis of non–reversible DC polarograms based on the Ružić's method (Equation 3.46), is given below:

$$I_{\mathrm{obs}} = \frac{I_{\mathrm{d}}}{\exp\tfrac{\alpha nF}{RT}(E_{\mathrm{appl}} - E^{irr}_{1/2}) + \exp\tfrac{nF}{RT}(E_{\mathrm{appl}} - E^{r}_{1/2}) + 1} + I_{\mathrm{b}} \qquad \textbf{(3.49)}$$

Parameters that are varied, in a nonlinear curve–fitting operation, using the Ružić DCP model given in Equation 3.49, to try to reproduce an experimental DC polarographic curve, are: I_{d}, α, $E^{r}_{1/2}$, $E^{irr}_{1/2}$, and parameters of the background current term I_{b}.

3.5.4 Concluding Remarks

The proposed nonlinear curve–fitting models for analysis of DC polarographic curves described in preceding sections were tested in this project in analysis of polarographic curves from complexation studies of Cd^{2+}, Pb^{2+}, and Zn^{2+} with the ligands sarcosine and glycine. The validity of the proposed models (to extract $E^{r}_{1/2}$ and I_d) is achieved by comparing stability constants obtained from the DC polarographic data to results obtained either from literature, and/or studied here by the independent technique of glass electrode potentiometry. The results obtained, and discussion related to the metal–ligand systems investigated in this work, have been provided in Chapter 5.

3.6 REFERENCES

1. D. Legett, ed., *Computational Methods for the Determination of Formation Constants*, New York: Plenum Press, **1985**, pp. 19–20.
2. H. Rossotti, *The Study of Ionic Equilibria: An Introduction*. New York: Longman, **1978**.
3. A. E. Martell and R. J. Motekaitis, *Coord. Chem. Rev.*, Vol. 100, **1990**, pp. 323–361.
4. G. H. Nancollas and M. B. Tomson, *Pure Appl. Chem.*, Vol. 54, **1982**, pp. 2676–2692.
5. E. Casassas, R. Tauler, and M. Filella, *Anal. Chim. Acta*, Vol. 191, **1986**, pp. 399–411.
6. P. M. May, K. Murray, and D. R. Williams, *Talanta*, Vol. 32, No. 6, **1985**, pp. 483–489.
7. P. M. May, K. Murray, and D. R. Williams, *Talanta*, Vol. 35, No. 11, **1985**, pp. 825–830.
8. P. M. May, K. Murray, and D. R. Williams, *Talanta*, Vol. 35, No. 12, **1988**, pp. 927–932.
9. I. Cukrowski and M. Adsetts, *J. Electroanal. Chem.*, Vol. 429, **1997**, pp. 129–137.
10. I. Cukrowski, *Electroanalysis*, Vol. 9, No. 15, **1997**, pp. 1167 –1173.
11. I. Cukrowski and S. A. Loader, *Electroanalysis*, Vol. 10, No.13, **1998**, pp. 877–885.
12. I. Cukrowski, R. D. Hancock, and R. C. Luckay, *Anal. Chim. Acta*, Vol. 319, **1996**, pp. 39–48.
13. I. Cukrowski, *Electroanalysis*, Vol. 11, No.9, **1999**, pp. 606–613.
14. I. Cukrowski, *J. Electroanal. Chem.*, Vol. 460, **1999**, pp. 197–206.
15. I. Cukrowski, and P. Franklyn, *3D Complex Formation Curves Package*, windows version 1.2.1, **2003**.
16. I. Cukrowski, *Anal. Chim. Acta*, Vol. 336, **1996**, pp. 23–36.
17. I. Cukrowski, J. R. Zeevart and N. V. Jarvis, *Anal. Chim. Acta*, Vol.379, **1999**, pp. 217–226.

18. R. D. Hancock, I. Cukrowski, I. Antunes, E. Cukrowska, J. Mashishi and K. Brown, *Polyhedron*, Vol. 14, No. 13–14, **1995**, pp. 1699–1707.
19. R. Luckay, R. D. Hancock, I. Cukrowski, and J. H. Reibenspeis, *Inorg. Chim. Acta*, Vol. 246, **1996**, pp. 159–169.
20. R. C. Luckay, I. Cukrowski, J. Mashishi, J. H. Reibenspies, A. H. Bond, R. D. Rogers, and R. D. Hancock, *J. Chem. Soc.*, *Dalton Trans.*, Vol. 5, **1997**, pp. 901–908.
21. I. Cukrowski, *Electroanalysis*, Vol. 9, No. 9, **1997**, pp. 699–705.
22. I. Cukrowski, *The Analyst*, Vol. 122, No.8, **1997**, pp. 827–833.
23. J. R. Zeevart, N. V. Jarvis, W. K. A. Louw, G. E. Jackson, I. Cukrowski and C. J. Mouton, *J. Inorg. Biochem.*, Vol. 73, No.4, **1999**, pp. 265–272.
24. I. Cukrowski and J. M. Zhang, *Electroanalysis*, Vol. 16, No. 8, **2004**, pp. 612–626.
25. I. Cukrowski, J. M. Zhang, and A. van Aswegen, *Helv. Chim. Acta*, Vol. 87, **2004**, pp. 2135–2158.
26. I. Cukrowski and J. M. Zhang, *Chem. Anal*. Vol. 50, **2005**, pp. 3–36.
27. A. M. Bond, *Modern Polarographic Methods in Analytical Chemistry*, New York: Marcell Dekker, **1980**.
28. D. R. Crow, *Polarography of Metal Complexes*, London: Academic Press, **1969**.
29. J. Heyrovský and J. Kůta, *Principles of Polarography*, New York and London: Academic Press, **1966**.
30. P. Delahay, *J. Am. Chem. Soc.*, Vol. 75, **1953**, pp. 1430 – 1435.
31. A. J. Bard and L. R. Faulkner, *Electrochemical Methods: Fundamentals and Applications*, New York: John Wiley & Sons, **2001**.
32. J. F. Rusling and T. F. Kumosinski, *Nonlinear Computer Modelling of Chemical and Biochemical Data*, London: Academic Press, **1996**.
33. G. Brink, *Precision Curve Fitter* version 1.08, Department of Chemistry, University of the Witwatersrand, Johannesburg.
34. H. Matsuda and Y. Ayabe, *Bull. Chem. Soc. Jpn.*, Vol. 28, **1955**, p. 422.
35. H. Matsuda and Y. Ayabe, *Bull. Chem. Soc. Jpn.*, Vol. 29, **1956**, p. 132.

36. H. Matsuda and Y. Ayabe, *Zeitschrift fur Elektrochemie*, Vol. 63, **1959**, pp. 1164–1171.
37. H. Matsuda and Y. Ayabe, *Zeitschrift fur Elektrochemie*, Vol. 66, **1962**, p. 469.
38. I. Ružić, A. Baric, and M. Branica, *J. Electroanal. Chem.*, Vol. 29, **1971**, pp. 411– 416.